REVIEW OF SCIENTIFIC INSTRUMENTS VOLUME 69, NUMBER 5 MAY 1998

Time and frequency-resolved photoluminescence up conversion using broadly tuneable picosecond infrared pulses

P. J. Poole[a)]
The Institute for Microstructural Sciences, National Research Council of Canada, Ottawa, K1A 0R6 Canada

J. Hong and Albert Stolow
The Steacie Institute for Molecular Sciences, National Research Council of Canada, Ottawa, Ottawa, Ontario, K1A 0R6 Canada

S. Charbonneau
The Institute for Microstructural Sciences, National Research Council of Canada, Ottawa, K1A 0R6 Canada

(Received 11 December 1997; accepted for publication 2 February 1998)

A simultaneous time and frequency-resolved photoluminescence setup based upon the concept of sum-frequency generation has been developed using the parallel collection capabilities of a liquid nitrogen cooled, high quantum efficiency charge coupled device (CCD) detector. This up conversion system can provide excellent time resolution (down to ~100 fs), when the detector is used in the single channel mode, with large dynamic range. When the CCD detector is used in its full capacity (1024 channels), wide spectral range as well as temporal information are obtained simultaneously from the up-converted signal, thus providing important information on the dynamics of various emission peaks which can occur simultaneously. Together with this, an efficient method for generation of high repetition rate, low energy infrared light between 1.44 and 1.62 μm is described. The technique uses difference frequency mixing of the fundamental wavelength of a mode-locked Nd:yttrium aluminum garnet laser and the output of a synchronously pumped Rhodamine 640 dye laser in a 10 mm long lithium triborate crystal. This source was then used to performed cw and time-resolved up-conversion photoluminescence measurements on a 1.54 μm emitting InGaAsP epitaxial layer. © *1998 American Institute of Physics.* [S0034-6748(98)03105=0]

I. INTRODUCTION

In the past decade, a range of advanced laser and associated optoelectronic instrumentation has emerged from specialized research laboratories to the general scientific and commercial marketplace to make possible spectroscopic studies of biological, chemical, and solid state systems by sophisticated methods in the picosecond and femtosecond time scale. More specifically to the solid state systems, there has been growing interest in the generation of tuneable infrared short pulses around 1.55 μm for applications such as optical communications, infrared time-resolved spectroscopy, and optical frequency mixing. This is particularly important in the investigation of the dynamics of fast semiconductor lasers and detectors operating at 1.55 μm, an important wavelength for telecommunications. A tuneable source allows resonant excitation of these structures, eliminating effects such as carrier screening when the photon energies are too large and carriers are generated away from the active region of the device. This allows the investigation of devices under the conditions in which they will be operated.

Time-resolved luminescence spectroscopy has provided important insight into the dynamical behavior of many semiconductor systems. With the advent of femtosecond lasers, the challenge for the luminescence spectroscopist is to develop techniques that can take full advantage of the ultrashort pulsewidths of these lasers.

Many different techniques have been used for obtaining time resolution in luminescence spectroscopy. An excellent review of the various techniques has been given by Fleming.[1] The most direct technique is to use a fast photomultiplier (PM) or a photodetector in conjunction with fast electronics. Using time-correlated single photon counting techniques in conjunction with fast PM tubes, it is possible to obtain a time resolution of better than 30 ps.[2]

The preferred technique for obtaining time resolution better than 100 ps has been to use a streak camera. Single shot streak cameras offer a time resolution better than 1 ps, but the inability to average signals over many laser pulses restricts them to strong signals.[3] Synchroscan streak cameras have become available, allowing signal averaging with a high repetition source, such as a mode-locked Ti:sapphire laser. However, this leads to some deterioration in the time resolution, with 10 ps being a practical limit for low level signals. A major drawback in the use of PM tubes and streak cameras is that the spectral response is limited by the spectral response of the photocathode, which typically does not extend beyond 1 μm.

The best hope for achieving luminescence time resolution comparable to the laser pulsewidth appears to be techniques that use nonlinearity induced by the laser pulse as a gate for luminescence. In this technique, called the up-

---

[a)]Electronic mail: philip.poole@nrc.ca

conversion technique[4] the luminescence excited by an ultrafast laser is mixed with the laser in a nonlinear crystal to generate sum frequency radiation. Since the mixing process takes place only during the presence of the laser pulse, this provides time resolution comparable to the laser pulsewidth.[5]

On the laser development front, recent advances in solid-state laser materials has shown that subpicosecond optical pulses of 1.39–1.55 μm can be produced by active mode-locked Cr:yttrium aluminum garnet (YAG) laser,[6] and Kerr-lens self-mode locked Cr:YAG lasers have demonstrated pulse widths down to 100 fs.[7,8] New dyes have also been synthesized for operating between 1.35 and 1.65 μm.[9] Optical parametric oscillators are presently the most employed way to provide wide tuneable wavelength light.[10,11] Here we have adopted the difference frequency mixing approach using lithium triborate (LBO) as the nonlinear medium, using a mode locked Nd:YAG laser and synchronous pumped dye laser as the excitation source. LBO has been particularly attractive in parametric applications due to its wide transparency range, high damage threshold, and large nonlinearity. A retracing phenomenon for both angle- and temperature-tuned phase matching schemes was reported by Lin *et al.*[12] It provides a useful technique for broadly tuneable short pulse systems and multiple wavelength generation.[13] The temperature phase matching retracing behavior causes the phase matching optical wavelength to no longer be monotonically related to the temperature. Thus operating near the temperature retracing point, effective broad tuning ability can be achieved.

The purpose of this article is to report on a broadly tuneable infrared photoluminescence (PL) up-conversion system used with a long wavelength tuneable laser source, allowing resonant optical excitation of structures in the 1.44–1.62 μm wavelength range. The time-resolved PL detection system is optimized to operate between 1 and 2 μm, and is capable of providing a time-resolution down to ~100 fs. It is based on a multichannel, liquid nitrogen cooled, high quantum efficiency charge coupled device (CCD) detector (SPEX Spectrum One). When the detector is used in the ''single'' channel mode, temporal information, such as radiative lifetime of particular transitions, can be extracted. However, when the CCD detector is used in its full capacity, i.e., as a multichannel detector, wide spectral range as well as temporal information (usually referred to as time windows[2]) are obtained simultaneously from the up-converted signal, thus providing important information on the dynamics of the various emission peaks which can occur simultaneously. The tuneable picosecond infrared generation is based on difference frequency mixing of the fundamental wavelength of a mode-locked Nd:YAG laser with the output of a synchronously pumped Rhodamine 640 dye laser in a 10-mm-long (LBO) crystal. This excitation source provides high repetition rate (76 MHz), low energy (pJ), tuneable (between 1.44 and 1.62 μm) radiation which can be use to performed both cw and time-resolved up-conversion PL measurements.

II. EXPERIMENTAL SETUP

The experimental setup for the generation of the tuneable infrared pulses is schematically represented in Fig. 1.

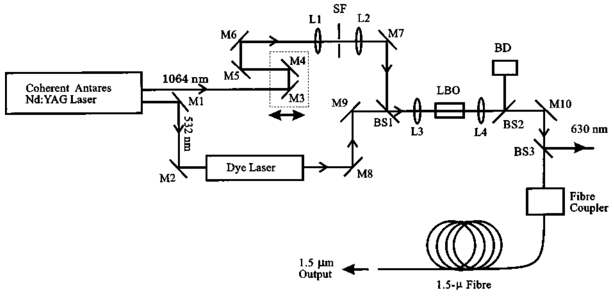

FIG. 1. Experimental setup utilized for difference frequency generation of infrared light by nonlinear mixing of the output of a dye laser and the fundamental output of a Nd:YAG laser. The dye laser is pumped by the frequency doubled output of the Nd:YAG laser and its output is superimposed on a dichroic mirror (BS1) with the residual fundamental light of the Nd:YAG laser. Subsequently both beams are focused down to a LBO crystal, where the difference frequency is generated, collimated, and the various wavelengths separated by a dichroic mirror (BS2,BS3). L1, L2, L3, and L4: 50-mm-focal length lenses; SF: spatial filter pinhole; BD: beam dump.

The main optical power source was a Coherent Antares cw mode-locked Nd:YAG laser. Its output was frequency doubled to synchronously pump a coherent 700 dye laser using Rhodamine 640 as the dye. The dye laser provided tuneable wavelengths from 610 to 650 nm with pulse widths typically of the order of 5 ps. Using an average power of 3 W at 532 nm, 600 mW of tuneable output could be generated from the dye laser, leaving about 15 W at the fundamental wavelength (1.064 μm) after doubling. The mode-locked Nd:YAG laser was run at 76 MHz, with optical pulses of 100 ps in width. In the 1.064 μm arm an optical delay line and a one to one telescope was inserted. A pin hole of 0.1 mm diameter was located close to the focal point of the telescope to eliminate scattered and deviated light caused by the Nd:YAG laser nonlinear doubling crystal. A half-wave plate was put in each beam for optimization of phase matching polarization. The two laser beams were collinear and used in the noncritical phase matching geometry. The nonlinear frequency conversion consisted of a 40-mm-focusing lens, a 10-mm-thick uncoated LBO crystal, and a 40-mm-collimating lens. Optimizing focal position inside the LBO crystal was achieved by adjusting the telescope. The crystal angle was not adjusted over the dye laser tuning range when characterizing the difference frequency generation in the LBO crystal (noncritical phase matching).

The generated infrared light was separated from the 1.064 μm and red beams by two successive dichroic mirrors. The first was highly reflecting at 1 μm with a high transmission in the red and 1.3–1.7 μm, while the second was a long wave pass filter with cut-off wavelength at 850 nm. A cross correlation, Fig. 2, was performed between the dye laser pulses and the generated infrared pulses by sum frequency generation in an angle tuned $LiIO_3$ crystal. The cross correlation gives a similar profile to that observed for the autocorrelation of the dye laser pulses [full width at half maximum (FWHM) of 9.3 ps], as expected for this infrared generation scheme.

Changing the dye laser wavelength without adjustment of the phase matching angle gave the tuning curve shown in Fig. 3(a). The calculated conversion efficiency of tuneable infrared power to the red pump power is plotted against the

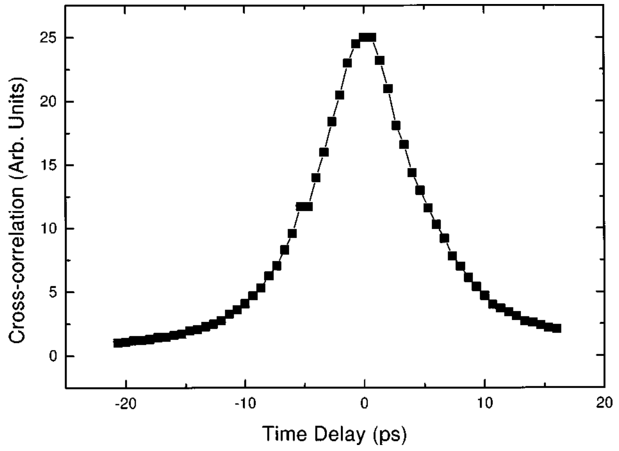

FIG. 2. Cross correlation of the 5 ps, 620 nm residual dye laser and the 5 ps, 1.5 μm generated. A full width at half maximum of 9.3 ps is obtained and corresponds to the instrumental time response of our detection system.

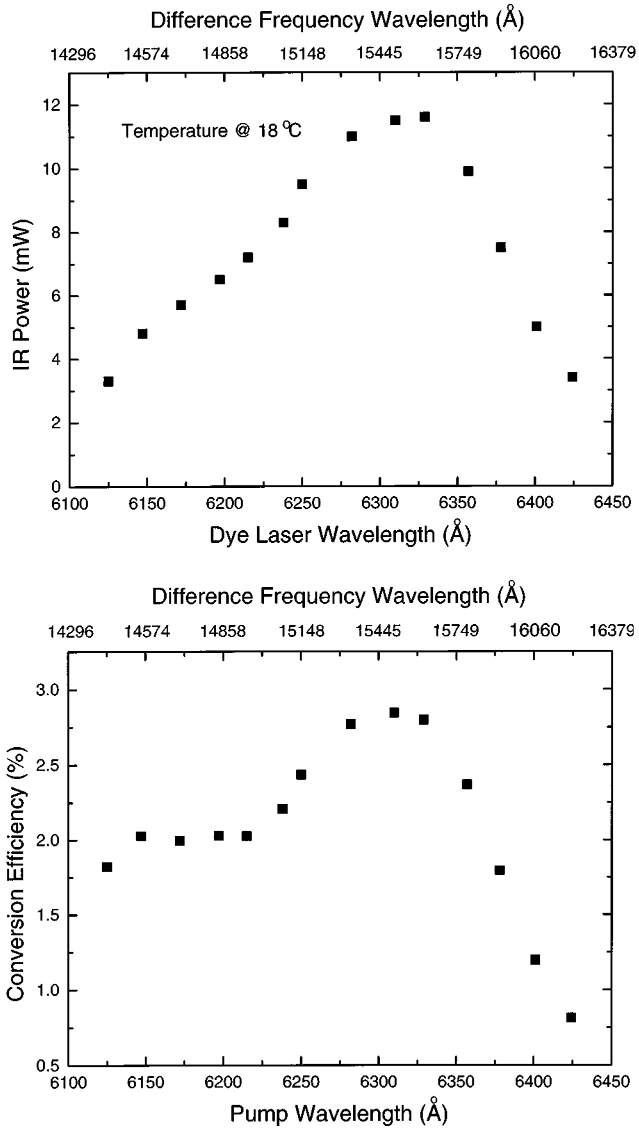

FIG. 3. (a) Tuning curve for the output of the IR light generated by mixing the Rhodamine 640 dye laser output in a LBO crystal with the residual 1.064 mm light from the Nd:YAG. The temperature of the crystal was constant at 18 °C. (b) Conversion efficiency obtained for the difference frequency mixing in the noncritical phase matching geometry.

pump wavelength in Fig. 3(b). The LBO crystal was held at 18 °C, near the temperature retracing point for the wavelength involved. The other mixed wavelength was kept at 1.064 μm throughout the tuning curve. The figure shows that the difference frequency generation bandwidth is wide enough to cover almost the whole tuning range of the Rhodamine 640 dye laser, even for the 10-mm-long LBO crystal at a fixed temperature. Further extension of phase matching wavelength range can be achieved by compromising the conversion efficiency through the use of a shorter nonlinear crystal. With a long crystal, in addition to the temporal pulse width, the generated difference frequency IR pulses will be affected by the group velocity mismatch (GVM) in the nonlinear crystal between the IR and dye laser pulses. The GVM between the two laser pulses is less important, however, due to the long pulse width of the Nd:YAG laser. In our case, some simple numerical calculations have shown that LBO is an excellent choice in this respect. For pulses at 1550 and 630 nm, the group velocity mismatch in a 10 mm LBO crystal amounts to 0.5 ps, which is still much less than the shortest laser pulse width.

Noncritical phase matching of this system provides a large acceptance angle and temperature bandwidth. For the 10 mm LBO crystal used in the present work, the calculated[14] acceptance angle and temperature bandwidth are 3.7–9.6 and 5.6–37.4 °C, respectively. The temperature dependence of the difference frequency mixing tuning curve is shown in Fig. 4 for a dye laser wavelength of 632.5 nm.

The experimental setup for the up-conversion system is shown schematically in Fig. 5. Following the difference frequency mixing scheme, described previously, the tuneable infrared pulses (1430–1670 nm) were used for the optical excitation (laser spot diameter $\sim 50\,\mu$m) of the samples, while the remaining visible pulses (610–650 nm) used as the optical gate. Luminescence from the sample is collected from a gold-coated, off-axis paraboloid mirror and focused ($\sim 50\,\mu$m diameter) on a 2-mm-thick $LiIO_3$ crystal (cut at 42°) with an identical off-axis paraboloid. The visible (610–650 nm) laser beam is delayed by a retroreflector located on a computer controlled delay stage (DS) and focused on the $LiIO_3$ crystal (C) to overlap the luminescence. The $LiIO_3$ crystal is located on a computer controlled rotation stage for optimizing the phase matching conditions. The luminescence and the laser are noncollinear. The sum frequency output is focused with a lens on the entrance slit of a 0.64 m spectrometer and detected by a Si CCD detector.

To demonstrate the suitability of the 1.5 μm tuneable pulse source for the spectroscopy of technologically relevant semiconductors, it was used as the excitation source for a cw and time-resolved PL experiment. After the generation and collimation of the 1.5 μm beam it was separated from the dye laser pulses using a dichroic beamsplitter and then coupled into a 1.5 μm multimode fiber. This allowed the source to be used anywhere within reach of the fiber and eliminated problems associated with atmospheric water absorption. The output of the fiber was then collimated and focused onto the sample to be investigated, a semiconductor

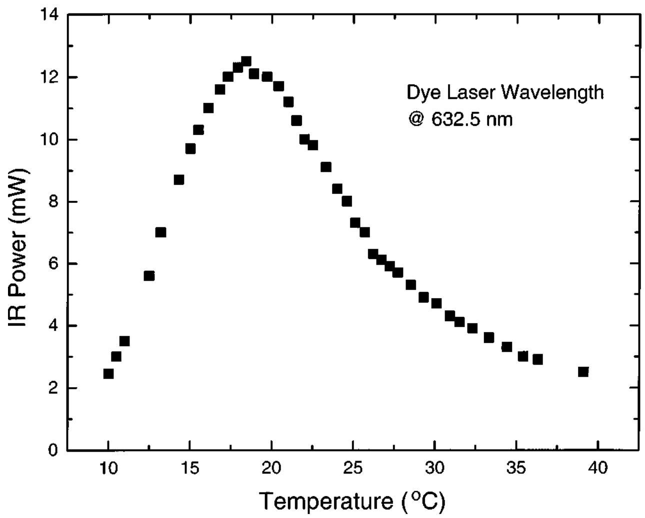

FIG. 4. Temperature dependence of the difference frequency mixing output at a dye laser wavelength of 632.5 nm in the noncritical phase matching geometry.

crystal consisting of a bulk InGaAsP epitaxial layer grown on InP, a material typically used for devices such as long wavelength laser diodes and detectors. This crystal was mounted in a liquid helium cryostat and held at a temperature of 4.2 K.

Figure 6 shows the steady state PL emission from the sample generated by 2 mW of power from the pulsed 1.5 μm excitation source as well as from a 2 mW cw HeNe laser. The PL setup used for these spectra consisted of a liquid nitrogen cooled germanium detector used in conjunction with a lock-in amplifier. Two features are observed in this figure, the first at 1.4985 μm is due to laser light scattered off the sample, the second centered at 1.54 μm is the PL from the bulk InGaAsP layer. The tuneable source allows us to tune from below to above the bandgap of the InGaAsP layer.

Time-resolved PL measurements on the InGaAsP sample were obtained using the up-conversion system discussed above. When the phase matching conditions are satisfied by angle tuning the $LiIO_3$ crystal, the sum frequency of the PL and the red dye laser are generated, in this case around 440 nm. By varying the delay of the red pulses relative to the 1.5 μm pulses exciting the sample, the temporal evolution of the PL could be mapped out, effectively performing a cross correlation between the PL and the red dye laser pulses. The time resolution of this system is governed primarily by two factors: the pulsewidth of the laser and the group velocity dispersion in the nonlinear crystal used for up-conversion, in this case $LiIO_3$. This imposes limitations on the thickness of the crystal for a given time resolution. Furthermore, since the efficiency of the up-converted signal decreases as the crystal thickness decreases, the ultimate time resolution attainable depends on the strength of the luminescence signal and the sensitivity of the detection system. It should also be pointed out that the limited up-conversion bandwidth of the nonlinear crystal can also broaden the time resolution. In the scheme used here, the time resolution was controlled by the pulse width of the laser sources used (the 1.5 μm and dye laser) and the jitter between them, which is expected to be negligible. Any dispersion in the optical apparatus will also degrade the time resolution, so paraboloid mirrors were used to collect the PL.

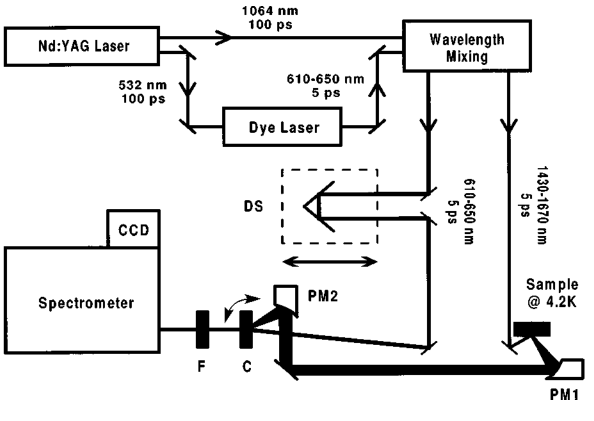

FIG. 5. Schematic representation of the time-resolved photoluminescence setup based on nonlinear frequency mixing depicting the laser system developed for resonant optical excitation (the details of which are presented in Fig. 1). The transient luminescence spectra and excitation pulses are subject to sum frequency generation in the nonlinear crystal (C), which acts as a fast nonlinear gate in the process. The luminescence is collected by nondispersive optics (PM1 and PM2 are off-axis paraboloid mirrors). DS=delay stage, F=filter, CCD=liquid nitrogen cooled charge coupled device (CCD camera).

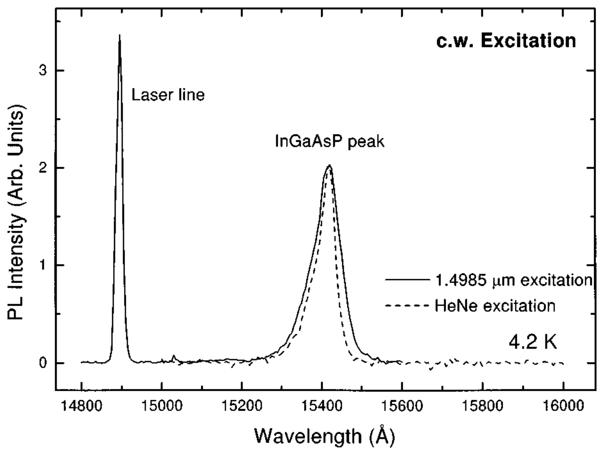

FIG. 6. Low temperature ($T=4.2$ K) steady-state PL emission spectra obtained on a 2-μm-thick InGaAsP epitaxial layer using a 2 mW cw HeNe laser for excitation (dash line) and the pulsed (5 ps, 76 MHz) difference frequency generated 1.4985 μm for excitation (full line).

Performing a cross correlation between the dye laser pulses and the scattered 1.5 μm pulses from the InGaAsP sample surface allows a determination of the temporal resolution of the system and the zero time delay. The measured cross correlation was 24 ps. The discrepancy between this result and the one obtained from Fig. 2 (9 ps) is due to the use of a multimode fiber for the IR pulses. Different optical modes in the fiber travel different distances, leading to a spread in the pulse width at the output of the fiber. The use of a single mode fiber would be expected to remove this effect resulting in a cross correlation of 9.3 ps.

If the luminescence spectrum is broad, the spectral resolution is determined by the spectral bandwidth of the nonlinear crystal. In order to obtain better spectral resolution, a spectrometer is usually used to disperse the up-converted

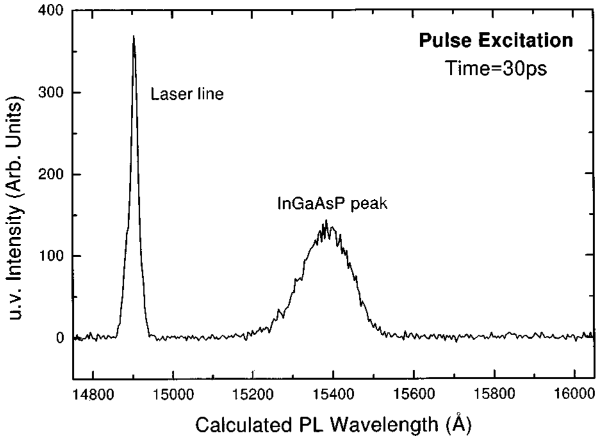

FIG. 7. Time-resolved PL spectrum of bulk InGaAsP obtained at a delay of 30 ps after the optical excitation. The time-window width, determined from the laser pulsewidth (after coupling in the multimode fiber), was 24 ps. The spectrum shows the laser line as well as the hot luminescence from the epitaxial layer.

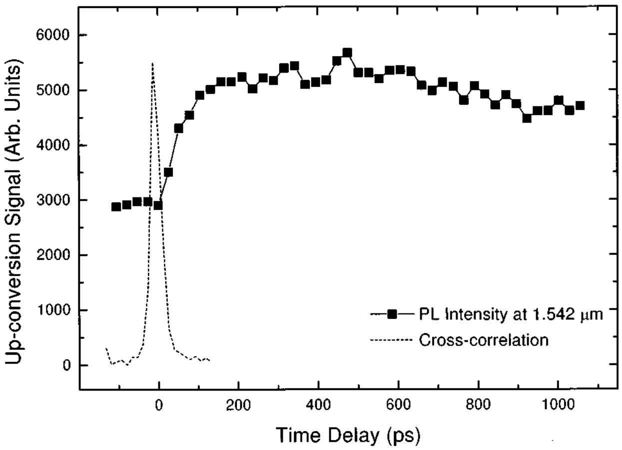

FIG. 8. Time evolution of the integrated PL emission of the bulk InGaAsP layer, and the cross correlation of the 620 nm dye laser with the 1.4985 μm laser light scattered off the sample surface. A full width at half maximum of 24 ps is obtained due to the use of multimode optical fiber and corresponds to the instrumental time response of our detection system.

signal, which is detected by a single channel detector such as a photomultiplier tube (PMT). However, the spectral bandwidth of the nonlinear crystal is generally larger than the desired spectral resolution but small compared to the spectral range of interest. In this case, one needs to vary the angle of the nonlinear crystal (due to phase matching conditions) to cover the entire spectral range, and the spectrometer wavelength has to be varied in synchronism with the crystal angle. However, if the single channel detector is replaced by a multiple channel CCD detector, and the crystal thickness as well as the laser pulse width are properly chosen, a complete spectrum can be integrated without scanning the spectrometer. Since the signal levels observed are generally very low, a multichannel detection system also has the advantage of decreasing the data collection time significantly.

With the spectrometer used here, the up-converted signal was dispersed on the cooled CCD camera allowing a full spectrum, with a spectral width of 32 nm centered at 440 nm, to be taken in a single shot. The advantage of using a CCD over a single channel photomultiplier tube is that spectral as well as temporal information is being collected simultaneously. This results in a very powerful spectroscopic system which combines the very low dark current and readout noise of the cooled CCD detector with simultaneous timing information about the individual photon events. The width of this temporal window is the same as the time resolution; i.e., 24 ps. This is demonstrated in Fig. 7, which displays a typical up-converted signal at a time delay of 30 ps from the InGaAsP sample. The wavelength scale has been converted from the UV wavelength back to the true PL wavelength (λ_{PL}) using the expression below:[4]

$$\frac{1}{\lambda_{\mathrm{PL}}}=\frac{1}{\lambda_{\mathrm{UV}}}-\frac{1}{\lambda_{\mathrm{laser}}},$$

where λ_{uv} is the detected up-converted wavelength, and λ_{laser} is the wavelength of the red dye laser pulses mixed with the PL to generate the up-conversion signal.

The spectrum in Fig. 7 looks very similar to the time integrated spectrum (Fig. 6). The phase matching bandwidth for the 2 mm crystal is large enough to cover the whole of the PL emission, and even reaches the excitation wavelength, although the efficiency is significantly reduced at this wavelength. By rotating the crystal, or by using a thinner one, the whole of the 32 nm UV detection range of the CCD for a set spectrometer position could be phase matched, allowing a complete spectrum to be taken with a single scan at a set delay. This allows direct measurements of the excited carrier temperatures to be made as a function of delay after excitation, providing insight into the carrier thermalization mechanisms. If a single channel system is used, e.g., a PMT, then the spectrometer has to be scanned as the crystal is rotated. The broadening observed in the PL InGaAsP emission peak taken at a delay of 30 ps (Fig. 7), when compared to the steady-state emission (Fig. 6), is simply a consequence of hot carrier recombination observed only at very short times.[15]

Figure 8 shows the time evolution of the up-converted PL signal at a wavelength corresponding to 1.542 μm for different time delays, with the cross correlation indicating zero time and the temporal resolution. The deconvolved risetime for the PL is 60 ps (using a measured risetime of 65 ps and cross correlation of 24 ps), and is due to the time taken for the excited carriers to cool down to the lattice temperature of 4.2 K. The initial excess energy given to an electron-hole pair is 28 meV (the difference between the laser energy and the bandgap of the InGaAsP) and corresponds to an electron temperature significantly higher than the lattice temperature of 4.2 K. After the PL intensity rises and reaches a maximum it slowly decays due to the decrease in carrier population through radiative and nonradiative loss mechanisms. The decay time is very long, >8 ns, as expected for good quality InGaAsP at 4.2 K.[15]

III. DISCUSSION

The experimental results presented in the preceding section show that difference frequency mixing in LBO allows the highly efficient generation of broadly tuneable IR light in the hard to access range of 1.44–1.62 μm. This was demonstrated using the output of a Nd:YAG pumped, visible dye laser and the residual fundamental output of the same Nd: YAG laser. Even though we have demonstrated this result for Rhodamine 640 dye, neighboring dyes will allow coverage of a greatly extended infrared range. Further increases in the power of the generated IR can also be obtained by the use of suitable antireflection coatings on the optics and crystal.

IV. CONCLUSIONS

In conclusion we have demonstrated a scheme for generating wavelength tuneable (1.44–1.6 μm) pulses at a high repetition rate (76 MHz) and an average power of typically 5 mW. This source was used to perform time averaged and time resolved PL measurements on a 1.54 μm emitting InGaAsP layer at 4.2 K. The use of a high quantum efficiency cooled CCD detector allowed the development of a very versatile time-windowing PL setup. The instrumental response function obtained using this technique is proportional to the pulsewidth used (~5 ps in this work). The primary advantages of this system are the huge parallel collection capabilities of the CCD detector reducing the time required to acquire an image and the simultaneous time resolution of the individual photon events.

ACKNOWLEDGMENT

A.S. and S.C. acknowledge the NRC Vice President Fund for financial support.

[1] G. R. Fleming and A. E. Siegman, in *Ultrafast Phenomena V*, edited by G. R. Fleming and A. E. Siegman (Springer, New York, 1986).
[2] S. Charbonneau, L. B. Allard, J. F. Young, G. Dyck, and B. J. Kyle, Rev. Sci. Instrum. **63**, 5315 (1992).
[3] W. Sibbett, SPIE Proceedings of the 15th International Congress on High Speed Photography and Photonics, 1982, Vol. **348**, p. 15.
[4] Jagdeep Shah, IEEE J. Quantum Electron. **24**, 276 (1988).
[5] H. Mahr and M. D. Hirch, Opt. Commun. **13**, 96 (1975).
[6] P. M. W. French, N. H. Rizvi, J. R. Taylor, and A. V. Shetakov, Opt. Lett. **18**, 39 (1993).
[7] P. J. Conlon, Y. P. Tong, P. M. W. French, J. R. Taylor, and A. V. Shestakov, Electron. Lett. **30**, 709 (1994).
[8] A. Sennaroglu, C. R. Pollock, and H. Nathel, Opt. Lett. **19**, 390 (1994).
[9] J. Zhang and Z. Zhu, Opt. Commun. **113**, 99 (1994).
[10] D. E. Spence, S. Wielandy, C. L. Tang, C. Bosshard, and P. Gunter, Opt. Lett. **20**, 680 (1995).
[11] M. Ebrahimzadeh, S. French, W. Sibbett, and A. Miller, Opt. Lett. **20**, 166 (1995).
[12] S. Lin, J. Y. Huang, J. Ling, C. Chen, and Y. R. Shen, Appl. Phys. Lett. **59**, 2805 (1991).
[13] J. Y. Zhang, J. Y. Huang, Y. R. Shen, and C. Chen, J. Opt. Soc. Am. B **10**, 1758 (1993).
[14] K. Kato, IEEE J. Quantum Electron. **QE-26**, 1173 (1990).
[15] K. Kash and J. Shah, J. Lumin. **30**, 333 (1985).